Robust Nonstationary Jammer Mitigation for GPS Receivers with Instantaneous Frequency Error Tolerance

Ben Wang[†‡], Yimin D. Zhang[‡], Si Qin[⋆] and Moeness G. Amin[⋆]

[†] College of Automation, Harbin Engineering University, Harbin, Heilongjiang 150001, China
[‡] Department of Electrical and Computer Engineering, Temple University, Philadelphia, PA 19122, USA
[⋆] Center for Advanced Communications, Villanova University, Villanova, PA 19085, USA

ABSTRACT

In this paper, we propose a nonstationary jammer suppression method for GPS receivers when the signals are sparsely sampled. Missing data samples induce noise-like artifacts in the time-frequency (TF) distribution and ambiguity function of the received signals, which lead to reduced capability and degraded performance in jammer signature estimation and excision. In the proposed method, a data-dependent TF kernel is utilized to mitigate the artifacts and sparse reconstruction methods are then applied to obtain instantaneous frequency (IF) estimation of the jammers. In addition, an error tolerance of the IF estimate is applied is applied to achieve robust jammer suppression performance in the presence of IF estimation inaccuracy.

Keywords: GNSS, GPS, jammer suppression, time-frequency analysis, compressive sensing, error tolerance

1. INTRODUCTION

Nonstationary jammer excision has been the subject of interest for anti-jam Global Positioning System (GPS) and Global Navigation Satellite System (GNSS) receivers for many years [1–3]. An important class of "smart" jammers assumes nonstationary frequency modulated (FM) waveforms, such as linear FM (LFM) or polynomial phase signal (PPS). Such "smart" jammers are characterized by their instantaneous frequencies (IFs). A number of anti-jam techniques have been proposed based on the above instantaneously narrowband signal characteristic [1,4–7], where joint-variable signal representations are used to reveal the jammer signature in the time-frequency (TF) domain. In this sense, jammer excision becomes a two-step process [8]: The first step is to estimate the TF signature or the IF of the jammer, whereas the second step is to perform excision based on the estimate of the jammer signatures. Both steps can be performed as a pre-processing prior to the correlation and dispreading loops of the GPS receivers.

Conventional GPS jammer suppression techniques, however, do not utilize the jammer sparsity, that is, the jammers only occupy a small number of TF points. In addition, these techniques assume the data to be sampled uniformly at the Nyquist or a higher sampling rate with all data samples available. This may not always be feasible in practice due to logistic constraints and propagation conditions. In [8], sparsity-based IF signature estimation and suppression of a single FM jammer are considered in a single-antenna GPS receiver. In this approach, the IF signature of a single jammer is estimated through sparse reconstruction by exploiting the fact that only a single frequency component is present in each time instant. In addition, the continuity of the IF signatures is exploited to further enhance the IF estimation capability and jammer suppression performance [9]. This technique is extended to multiple-sensor platforms for multiple-jammer suppression in [7,10].

Effective anti-jam techniques require accurate IF estimation. In practice, however, the estimated IF may not be sufficiently accurate due to, e.g., noise, interference, and frequency discretization. The IF estimation accuracy is further compromised when the observed data contain missing samples due, among other reasons, to gating of highly corrupted noisy samples. Incomplete data observations cause undesirable artifacts in the TF domain.

In this paper, we consider robust jammer suppression in such challenging situations. We first apply a data-dependent TF kernel to mitigate the effect of artifacts due to missing samples, and the sparse reconstruction

Contact information: ydzhang@temple.edu.

techniques are then exploited to estimate the IFs of the jammers. Jammer removal is achieved by projecting a segmented received signals to the orthogonal subspace of the estimated jammer subspace. In particular, we achieve robust jammer suppression in the presence of inaccurate IF estimation by broadening the jammer IF signatures in the TF domain when the orthogonal projection is applied.

Notations: We use lower-case (upper-case) bold characters to denote vectors (matrices). In particular, $\mathbf{I}_N$ denotes the $N \times N$ identity matrix. $(.)^*$ denotes complex conjugation, and $(\cdot)^T$ and $(\cdot)^H$, respectively, stand for transpose and Hermitian operations. $\mathcal{F}_x$ and $\mathcal{F}_x^{-1}$ respectively denote discrete Fourier transform (DFT) and inverse DFT (IDFT) matrices with respect to x. $\mathcal{CN}(a, b)$ denotes a complex Gaussian distribution with mean a and variance b. In addition, $\delta(x)$ represents the Dirac delta function of x, $\bigotimes$ denotes the Kronecker product, and $\jmath = \sqrt{-1}$.

2. SIGNAL MODEL

Consider a scenario that Q narrowband GPS signals in the presence of H narrowband FM jammers. Then, the received time signal can be expressed as

$$y(t) = \sum_{i=1}^{Q} s_i(t) + \sum_{j=1}^{H} h_j(t) + n(t), \tag{1}$$

where $s_i(t)$ and $h_j(t)$ are the waveforms of the ith GPS and the jth jammer signal, respectively. In addition, $n(t)$ is the additive white complex Gaussian noise with $\mathcal{CN}(0, \sigma_n^2)$.

Denote $x(t)$ as the sparse observations with M_r missing samples, where $0 \leq M_r < T$. The missing positions are assumed to be randomly and uniformly distributed over time. As such, $x(t)$ behaves as the product of the received signal $y(t)$ and the observation mask $b(t)$, expressed as

$$x(t) = y(t) \cdot b(t), \tag{2}$$

where

$$b(t) = \begin{cases} 1, & \text{if } t \in \mathcal{S}, \\ 0, & \text{if } t \notin \mathcal{S}, \end{cases}$$

and $\mathcal{S}$ denotes the index set of nonzero elements of $b(t)$. The cardinality of $\mathcal{S}$ is $|\mathcal{S}| = T - M_r$.

3. TIME-FREQUENCY REPRESENTATIONS AND SPARSE RECONSTRUCTION

In this section, we briefly discuss bilinear time-frequency distribution (TFD), TF kernel, and the sparse reconstruction of TF signal representation (TFSR) [11–15].

3.1 Wigner-Ville Distribution

For FM signals, we can exploit the TFD to characterize the time-varying IF signatures with respect to the time samples. A general class of bilinear TFSR of signal $x(t)$ can be obtained under the Cohen's class. The Wigner-Ville distribution (WVD), expressed as [11, 12]:

$$D(t, f) = \mathcal{F}_\theta^{-1}\{\mathcal{F}_\tau(A(\theta, \tau))\}, \tag{3}$$

is often regarded as the prototype of the Cohen's class TFSR, where

$$A(\theta, \tau) = \int_{-\infty}^{\infty} x\left(t + \frac{\tau}{2}\right) x^*\left(t - \frac{\tau}{2}\right) e^{-\jmath 2\pi\theta t} dt \tag{4}$$

is the ambiguity function (AF) of $x(t)$, with θ and τ, respectively, denoting the frequency shift and the time lag. In addition, $C(t, \tau)$ expressed below is referred to as the instantaneous autocorrelation function (IAF) of signal $x(t)$:

$$C(t, \tau) = x\left(t + \frac{\tau}{2}\right) x^*\left(t - \frac{\tau}{2}\right). \tag{5}$$

Therefore, the AF $A(\theta,\tau)$ is the one-dimensional (1-D) DFT of the IAF $C(t,\tau)$ with respect to time variable t. On the other hand, the WVD $D(t,f)$ is the 1-D DFT of the IAF $C(t,\tau)$ with respect to time lag τ, and the two-dimensional (2-D) DFT of AF $A(\theta,\tau)$.

It is known that WVD provides a high resolution when the signals are LFM. However, due to its bilinear nature, it generally suffers from cross-terms when the signals are not simple LFM waveforms or contain multiple signal components. In addition, when the signals are sparsely sampled, the WVD also suffers from artifacts due to missing samples.

3.2 Adaptive Optimal Kernel

The effect of artifacts due to missing data can be mitigated through a proper TF kernel [14]. A TF kernel is represented as a multiplying mask matrix in the ambiguity domain and was traditionally considered as an effective means for cross-term suppression based on the fact that the majority of auto-term TFDs are located near the origin in the ambiguity domain, whereas the cross-terms are distant from the time lag and frequency shift axes. This property has motivated researchers to develop reduced-interference distribution kernels with low-pass filter characteristics in the ambiguity domain to suppress cross-terms and preserve auto-terms. Because the effect of the artifacts due to missing samples resembles that of the noise in the sense that it spreads over the entire TF region, TF kernels are also effective for artifact mitigation.

In this paper, we use the adaptive optimal kernel (AOK) [13] for this purpose with a signal-adaptive filtering capability. The AOK is obtained by solving the following optimization problem

$$\begin{aligned} &\max_{\Phi} \int_0^{2\pi}\int_0^{\infty} \left|A(r,\psi)\Phi(r,\psi)\right|^2 r dr d\psi \\ &\text{subject to} \quad \Phi(r,\psi) = \exp\left(-\frac{r^2}{2\sigma(\psi)}\right), \\ &\qquad\qquad \frac{1}{4\pi^2}\int_0^{2\pi}\sigma(\psi)d\psi \le \alpha, \end{aligned} \tag{6}$$

where $A(r,\psi)$ denotes the AF of the received signal $x(t)$ and Φ denotes a matrix with all $\Phi(r,\psi)$ entries, both are defined in the polar coordinate with radius r and angle ψ. The Gaussian constraint in $\Phi(r,\psi)$ leads to cross-term reduction. Parameter $\alpha \ge 0$ is a volume constraint that tradeoffs between cross-term suppression and auto-term preservation.

3.3 Sparse Reconstruction of TFSR

Utilizing the TF kernel obtained from (6), the TFD of the received signal can be computed as the 2-D DFT of the kernelled AF, $A(r,\psi)\Phi(r,\psi)$. Converting the kernelled AF to rectangular coordinate system, and denoting the result as $\tilde{A}(\theta,\tau)$, the corresponding kernelled TFD is expressed as

$$D(t,f) = \mathcal{F}_{\theta}^{-1}\{\mathcal{F}_{\tau}[\tilde{A}(\theta,\tau)]\}. \tag{7}$$

Alternative to performing 2-D DFT, we can obtain the TFD through sparse reconstruction from the AF matrix $\tilde{\mathbf{A}}$, which collects $\tilde{A}(\theta,\tau)$ for all θ and τ as its elements. In this case, rather than utilizing the 2-D DFT relationship between the AF and the TFD as in [16, 17], it is shown in [9, 14] that the 1-D DFT relationship between the IAF and the TFD yields simpler computations and, more importantly, enables the exploitation of local sparsity in the TF domain with respect to each time instant t.

The 1-D IDFT of $\tilde{A}(\theta,\tau)$ with respect to θ yielding the kernelled IAF,

$$C(t,\tau) = \mathcal{F}_{\theta}^{-1}\{\tilde{A}(\theta,\tau)\}. \tag{8}$$

Denote $\mathbf{c}^{[t]}$ as a column vector that contains all elements of $C(t,\tau)$ for all τ and a specific time instant t, and $\mathbf{w}^{[t]}$ as a vector corresponding to the t-th column of TFD matrix $\tilde{\mathbf{D}}$, $t = 0, \cdots, T-1$. Then, these two vectors are related by

$$\mathbf{c}^{[t]} = \mathbf{\Psi}\mathbf{w}^{[t]} + \boldsymbol{\varepsilon}^{[t]}, \tag{9}$$

where $\mathbf{\Psi}$ is the 1-D IDFT matrix. Because the IF of the jammer is sparse in frequency domain corresponding to each constant t, the non-zero entries of $\mathbf{w}^{[t]}$ in (9) can be reconstructed through a sparse reconstruction techniques. In this case, the sparse reconstruction problem is formulated as

$$\begin{array}{ll} \min & ||\mathbf{w}^{[t]}||_1 \\ \text{s.t.} & ||\mathbf{c}^{[t]} - \mathbf{\Psi}\mathbf{w}^{[t]}|| < \delta, \end{array} \tag{10}$$

where δ is a user-specific parameter.

A number of sparse reconstruction algorithms can be used to solve the above problem, such as OMP, Lasso and Bayesian compressive sensing [18–21]. In this paper, we utilize the OMP algorithm to perform sparse reconstruction of the TFSR.

4. JAMMER SUPPRESSION WITH EXTENDED ESTIMATION FREQUENCY

In this section, we first briefly review the conventional orthogonal projection scheme for jammer suppression technique [8] and then present a new approach based on the frequency extension.

4.1 Jammer Suppression Technique

Define IFs of the jammer signals $f(t)$ as the derivative of the phase $\varphi(t)$, i.e.,

$$f(t) = \frac{1}{2\pi}\frac{d\varphi(t)}{dt}. \tag{11}$$

Thus, the jammer phase information can be reconstructed through the integration of the estimated IF $\hat{f}(t)$ except the initial phase, provided that the IFs of jammer signals are estimated. Then, the estimated temporal signature of the j-th jammer can be expressed as

$$\hat{\mathbf{h}}_j = [\hat{h}_j(0), \cdots, \hat{h}_j(T-1)]^T, \tag{12}$$

where $\hat{h}_j(t) = \exp(\jmath\hat{\varphi}_j(t))$, and $\hat{\varphi}(t)$ is the estimated phase of the jth jammer signal. Denote $\mathbf{V} = [\hat{\mathbf{h}}_1, \cdots, \hat{\mathbf{h}}_H]$ as the overall subspace of the interference. The projection matrix into the orthogonal subspace of the jammers is given by [6]

$$\mathbf{P} = \mathbf{I}_T - \mathbf{V}\left(\mathbf{V}^H\mathbf{V}\right)^{-1}\mathbf{V}^H. \tag{13}$$

As such, the jammer-suppressed time-domain samples are expressed as the following $T \times 1$ vector

$$\hat{\mathbf{x}} = \mathbf{P}\tilde{\mathbf{x}}, \tag{14}$$

where $\tilde{\mathbf{x}} = [x^T(0), \cdots, x^T(T-1)]^T$ is the received signal vector.

4.2 Jammer Instantaneous Frequency Error Tolerance

The orthogonal projection scheme for jammer suppression, as described above, is highly dependent on the subspace construction. That is, an accurate phase estimation of signals is required to achieve effective jammer suppression. However, the estimated IFs $\hat{f}_j(t), j = 1, \cdots, H$, may not be sufficiently accurate due to, e.g., noise perturbation and frequency discretization error. As such, the error will be accumulated with time in the integration process to estimate the phase information. In this case, the conventional technique suffers significant performance degradation. Note that, for each time instant t, the majority of the jammer power is concentrated nearby the respective jammer IF estimates. Inaccuracies in IF estimation can be accounted for by including all IFs within a predefined instantaneous bandwidth [11].

Denote the augmented IF signatures of the jth jammer signal as

$$\hat{\mathbf{f}}_j^w(t) = \left[\hat{f}_j^{-M}(t), \cdots, \hat{f}_j^0(t), \cdots, \hat{f}_j^M(t)\right], \tag{15}$$

where $\hat{f}_j^m(t) = \hat{f}_j(t) + m\Delta f, m \in \{-M, \cdots, 0, \cdots, M\}$, Δf is the frequency increment, and M is number of added frequency components in each side of the spectrum. The total number of frequency components after IF augmentation becomes $2M + 1$ for each jammer signal.

The augmented phase signatures for the jth jammer signal can be calculated by integrating the augmented IF signatures in (15)

$$\hat{\boldsymbol{\varphi}}_j^w(t) = 2\pi \int_0^t \hat{\mathbf{f}}_j^w(\tau) d\tau. \tag{16}$$

Thus, the reconstructed jth jammer signal corresponding to the augmented frequencies can be expressed as

$$\hat{\mathbf{H}}_j^w = [\mathbf{d}_j^{-M}, \cdots, \mathbf{d}_j^0, \cdots, \mathbf{d}_j^M], \tag{17}$$

where $\mathbf{d}_j^m = [d_j^m(0), \cdots, d_j^m(T-1)]^T$ with $d_j^m(t) = \exp(\jmath\hat{\varphi}_j^m(t))$. As such, the subspace of the H jammer signals can be expressed as

$$\tilde{\mathbf{V}} = \left[\hat{\mathbf{H}}_1^w, \cdots, \hat{\mathbf{H}}_H^w\right]. \tag{18}$$

Then, the projection matrix into the orthogonal subspace of the augmented jammer subspace becomes

$$\tilde{\mathbf{P}} = \mathbf{I}_T - \tilde{\mathbf{V}}(\tilde{\mathbf{V}}^H\tilde{\mathbf{V}})^{-1}\tilde{\mathbf{V}}^H. \tag{19}$$

It is noted that, while the augmented jammer IF signatures introduces some additional GPS signal loss, such effect is practically negligible because of the high dimension used in the orthogonal projection.

5. SIMULATION RESULTS

For illustrative purposes, we consider two FM jammers impinging on the receiver along with an L1 band GPS signals with C/A codes. The chip rate of the signals is 1.023 MHz, and the IF laws of the two jammers are assumed to be

$$\begin{aligned} f_1(t) &= 0.05 + 0.05t/T + 0.1t^2/T^2, \\ f_2(t) &= 0.15 + 0.05t/T + 0.1t^2/T^2, \end{aligned} \tag{20}$$

for $t = 0, \cdots, T-1$ and $T = 256$. The signal-to-noise ratio (SNR) of the GPS waveform is -16 dB and the input jammer-to-noise ratio (JNR) is assumed to be 25 dB. In addition, we assume that 50% of data samples are randomly missing, i.e., $M_r = 128$.

When constructing the sparse TFSR, the number of frequencies is set to 1024, and the yielding frequency resolution is approximately 1 KHz. We use $M = 5$, i.e., the dimension of the augmented IF signature is 11 for each jammer. Δf is chosen to be 20% of the frequency resolution (or approximately 200 Hz), and the augmented signatures thus occupy a total bandwidth of 2 KHz centered at the estimated frequency.

In Figure 1, one realization of the real-part of the jammed GPS signal waveform with missing samples is presented, where the red dots represent the 128 missing samples.

The WVD of the jamed GPS signal is shown in Figure 2(a). It is observed that the WVD suffers from the artifacts missing data samples as well as cross-terms. As a consequence, it becomes difficult to accurately estimate the IFs of the jammer signals from this result. To suppress the effect of artifacts, we apply the AOK in the TFD computation, and the corresponding IF estimate is obtained through sparse reconstruction using the OMP algorithm. The resulting TFSR is shown in Figure 2(b). It is apparent that the reconstructed result is well approximated as the true IF signatures. Figures 2(c) and 2(d) show the WVD after jammer suppression using the conventional method without IF signature augmentation and the proposed method with IF augmentation, respectively. The results depicted in Figure 2(c) show imperfect jammer suppression. On the other hand, jammer signals are effectively suppressed in the results presented in Figure 2(d), demonstrating the effectiveness of the proposed method.

In Figure 3, we compare the averaged output signal-to-jammer-plus-noise ratio (SJNR) of different methods as a function of the input JNR, where the results are obtained by averaging 100 independent trails. The advantages of the proposed method over conventional approach in achieving a higher output SJNR are clearly demonstrated.

6. CONCLUSION

In this paper, we proposed a nonstationary jammer suppression method for GPS receivers when the signals are sparsely sampled. In addition to using a data-dependent TF kernel to mitigate the artifacts and exploit sparse reconstruction for jammer IF signature estimation, the main contribution of this paper is to use augmented jammer IF signatures to achieve robust jammer suppression in the presence of jammer IF estimation inaccuracy. The effectiveness of the proposed approach is verified using simulation results.

REFERENCES

[1] Y. Zhang, M. G. Amin, and A. R. Lindsey, "Anti-jamming GPS receivers based on bilinear signal distributions," in *Proc. IEEE Military Communications Conf.*, Vienna, VA, Oct. 2001, pp. 1070–1074.

[2] Y. D. Zhang and M. G. Amin, "Anti-jamming GPS receiver with reduced phase distortions," *IEEE Signal Processing Letters*, vol. 19, no. 10, pp. 635–638, Oct. 2012.

[3] M. G. Amin, X. Wang, Y. D. Zhang, F. Ahmad, and E. Aboutanios, "Sparse array and sampling for interference mitigation and DOA estimation in GNSS," *Proc. IEEE* (in press).

[4] M. G. Amin and A. Akensu, "Time-frequency for interference excision in spread spectrum communications," *IEEE Signal Processing Magzine*, vol. 16, no. 2, March 1999.

[5] S. Barbarossa and A. Scaglione, "Adaptive time-varying cancellation of wideband interferences in spread-spectrum communications based on time-frequency distributions," *IEEE Trans. Signal Process.*, vol. 47, pp. 957–965, April 1999

[6] Y. Zhang and M. G. Amin, "Array processing for nonstationary interference suppression in DS/SS communications using subspace projection techniques," *IEEE Trans. Signal Process.*, vol. 49, no. 12, pp. 3005–3014, December 2001.

[7] Y. D. Zhang, M. G. Amin, and B. Wang, "Mitigation of sparsely sampled nonstationary jammers for multi-antenna GNSS receivers," in *Proc. IEEE ICASSP*, Shanghai, China, March 2016.

[8] M. G. Amin and Y. D. Zhang, "Nonstationary jammer excision for GPS receivers using sparse reconstruction techniques," in *Proc. ION GNSS+*, Tampa, FL, Sept. 2014, pp. 3469–3474.

[9] Q. Wu, Y. D. Zhang, and M. G. Amin, "Continuous structure based Bayesian compressive sensing for sparse reconstruction of time-frequency distribution," in *Proc. Int Conf. Digital Signal Process.*, Hong Kong, China, Aug. 2014, pp. 831–836.

[10] Y. D. Zhang, B. Wang, and M. G. Amin, "Multi-sensor excision of sparsely sampled nonstationary jammers for GPS receivers," in *Proc. ION GNSS+*, Tampa, FL, Sept. 2015, pp. 3284–3288.

[11] L. Cohen, *Time Frequency Analysis: Theory and Applications.* Prentice Hall, 1995.

[12] B. Boashash (ed.), *Time-Frequency Signal Analysis and Processing, 2nd Ed.* Academic Press, 2015.

[13] R. G. Baraniuk and D. L. Jones, "A signal-dependent time-frequency representation: optimal kernel design," *IEEE Trans. Signal Process.*, vol. 41, no. 4, pp. 1589–1602, April 1993.

[14] Y. D. Zhang, M. G. Amin, and B. Himed, "Reduced interference time-frequency representations and sparse reconstruction of undersampled data," in *Proc. EUSIPCO*, Marrakech, Morocco, Sept. 2013, pp. 1–5.

[15] M. G. Amin, B. Jakonovic, Y. D. Zhang, and F. Ahmad, "A sparsity-perspective to quadratic time-frequency distributions," *Digital Signal Process.*, vol. 46, pp. 175–190, Nov. 2015.

[16] P. Flandrin and P. Borgnat, "Time-frequency energy distributions meet compressed sensing," *IEEE Trans. Signal Process.*, vol. 58, no. 6, pp. 2974-2982, 2010.

[17] Y. D. Zhang and M. G. Amin, "Compressive sensing in nonstationary array processing using bilinear transforms," in *Proc. IEEE SAM Workshop*, Hoboken, NJ, June 2012, pp. 349–352.

[18] J. A. Tropp and A. C. Gilbert, "Signal recovery from partial information via orthogonal matching pursuit," *IEEE Trans. Info. Theory*, vol. 53, no. 12, pp. 4655-4666, 2007.

[19] R. Tibshirani, "Regression shrinkage and selection via the Lasso," *J. Royal Statist. Soc.*, vol. 58, no. 1, pp. 267-288, 1996.

[20] S. Ji, D. Dunson, and L. Carin, "Multi-task compressive sampling," *IEEE Trans. Signal Process.*, vol. 57, no. 1, pp. 92-106, 2009.

[21] Q. Wu, Y. D. Zhang, M. G. Amin, and B. Himed, "Complex multitask Bayesian compressive sensing," in *Proc. IEEE ICASSP*, Florence, Italy, May 2014, pp. 3375–3379.

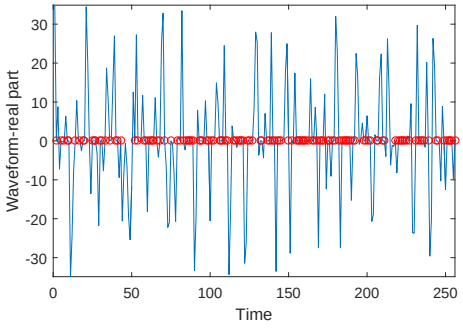

Figure 1: Waveform with missing samples.

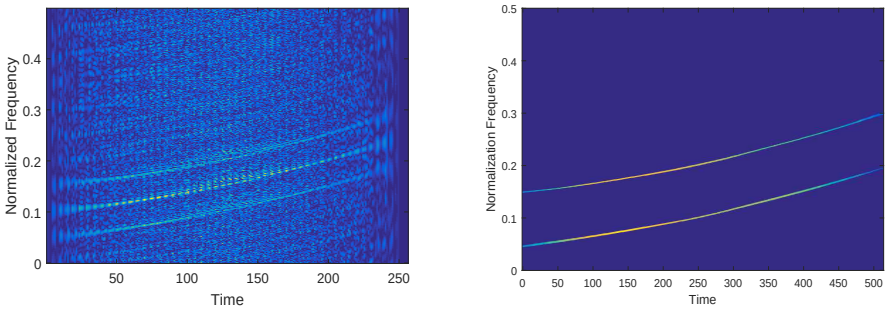

Figure 2: TFD results. (a) WVD of the jammed GPS signal; (b) Reconstructed TFSR from OMP; (c) WVD of GPS signal after jammer suppression without IF signature augmentation; (d) WVD of GPS signal after jammer suppression using the proposed method with jammer IF signature augmentation.

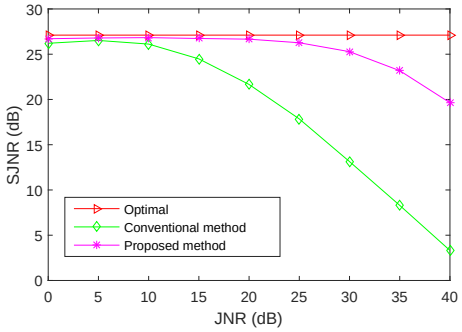

Figure 3: Output SJNR versus input JNR.